
AlphaDesign: A graph protein design method and benchmark on AlphaFoldDB

Zhangyang Gao^{*1,2} Cheng Tan^{*1,2} Stan Z. Li¹

Abstract

While DeepMind has tentatively solved protein folding, its inverse problem – protein design which predicts protein sequences from their 3D structures – still faces significant challenges. Particularly, the lack of large-scale standardized benchmark and poor accuracy hinder the research progress. In order to standardize comparisons and draw more research interest, we use AlphaFold DB, one of the world’s largest protein structure databases, to establish a new graph-based benchmark – AlphaDesign. Based on AlphaDesign, we propose a new method called ADesign to improve accuracy by introducing protein angles as new features, using a simplified graph transformer encoder (SGT), and proposing a confidence-aware protein decoder (CPD). Meanwhile, SGT and CPD also improve model efficiency by simplifying the training and testing procedures. Experiments show that ADesign significantly outperforms previous graph models, e.g., the average accuracy is improved by 8%, and the inference speed is 40+ times faster than before.

1. Introduction

As “life machines,” proteins play vital roles in almost all cellular processes, such as transcription, translation, signaling, and cell cycle control. Understanding the relationship between protein structures and their sequences brings significant scientific impacts and social benefits in many fields, such as bioenergy, medicine, and agriculture (Huo et al., 2011; Williams et al., 2019). While AlphaFold2 (Jumper et al., 2021) has tentatively solved protein folding from 1D sequences to 3D structures, its reverse problem, i.e., protein design raised by (Pabo, 1983) that aims to predict amino acid sequences from known 3D structures, has fewer breakthroughs in the ML community. The main reasons hindering the research progress include: (1) The lack of large-scale standardized benchmarks; (2) The difficulty in improving protein design accuracy; (3) Many methods are neither efficient nor open source. Therefore, a crucial question grips

our heart: How to benchmark protein design and develop an effective and efficient open-sourced method?

Previous benchmarks may suffer from biased testing and unfair comparisons. Since SPIN (Li et al., 2014) introduced the TS50 consisting of 50 native structures, it has been served as a common test set for evaluating different methods (O’Connell et al., 2018; Wang et al., 2018; Chen et al., 2019; Jing et al., 2020; Zhang et al., 2020a; Qi & Zhang, 2020; Strokach et al., 2020). However, such a few proteins do not cover the vast protein space and are more likely to lead to biased tests. Besides, there are no canonical training and validation sets, which means that different methods may use various training sets. If the training data is inconsistent, how can we convince researchers that the performance gain comes from the difference of methods rather than data? Especially when the test set is small, adding training samples that match the test set distribution may dramatic performance fluctuations. For fair comparisons, how to establish a large-scale standardized benchmark?

Extracting expressive residue representations is a key challenge for accurate protein design, where both sequential and structural properties need to be considered. For general 3D points, structural features should be rotationally and translationally invariant in the classification task. Regarding proteins, we should further consider the regular structure, number, and order of amino acids. Previous studies (O’Connell et al., 2018; Wang et al., 2018; Ingraham et al., 2019; Jing et al., 2020) may have overlooked some important protein features and better model designs; thus, none of them exceed 50% accuracy except DenseCPD (Qi & Zhang, 2020). For higher accuracy, how to construct better protein features and neural models to learn expressive residue representations?

Improving the model efficiency is necessary for rapid iteration of researches and applications. Current advanced GNN and CNN methods have severe speed defects due to the sequential prediction paradigm. For example, GraphTrans (Ingraham et al., 2019) and GVP (Jing et al., 2020) predict residues one by one during inference rather than in parallel, which means that it calls the model multiple times to get the entire protein sequence. Moreover, DenseCPD (Qi & Zhang, 2020) takes 7 minutes to predict a 120-length protein on their server¹. How can we improve the model efficiency while ensuring accuracy?

^{*}Equal contribution ¹AI Research and Innovation Lab, Westlake University ²Zhejiang University. Correspondence to: Stan Z. Li <Stan.ZQ.Li@westlake.edu.cn>.

¹<http://protein.org.cn/densecpd.html>

To address these problems, we establish a new protein design benchmark – AlphaDesign, and develop a graph model called ADesign to achieve SOTA accuracy and efficiency. Firstly, AlphaDesign compares various graph models on consistent training, validation, and testing sets, where all these datasets come from the AlphaFold Protein Structure Database (Varadi et al., 2021). In contrast to previous studies (Ingraham et al., 2019; Jing et al., 2020) that use limited-length proteins and do not distinguish species, we extend the experimental setups to length-free and species-aware. Secondly, we improve the model accuracy by introducing protein angles as new features, using a simplified graph transformer encoder (SGT), and proposing a constraint-aware protein decoder (CPD). Thirdly, SGT and CPD also improve model efficiency by simplifying the training and testing procedures. Experiments show that ADesign significantly outperforms previous methods in both accuracy (+8%) and efficiency (40+ times faster than before).

2. Related work

We focus on structure-based protein design, and the mainstream approaches can be categorized into three groups, i.e., MLP-based, CNN-based, and GNN-based methods. Some terms need to be explained in advance: we call amino acids in the protein as residues, and accuracy is an indicator of how well the residues predict.

Problem definition The structure-based protein design aims to find the amino acids sequence $\mathcal{S} = \{s_i : 1 \leq i \leq n\}$ that folds into a known 3D structure $\mathcal{X} = \{\mathbf{x}_i \in \mathbb{R}^3 : 1 \leq i \leq n\}$, where n is the number of residues and the natural proteins are composed by 20 types of amino acids, i.e., $1 \leq s_i \leq 20$. Formally, that is to learn a function \mathcal{F}_θ :

$$\mathcal{F}_\theta : \mathcal{X} \mapsto \mathcal{S}. \quad (1)$$

Because homologous proteins always share similar structures (Pearson & Sierk, 2005), the problem itself is under-determined, i.e., the valid amino acid sequence may not be unique. In addition, the need to consider both 1D sequential and 3D structural information further increases the difficulty of algorithm design. As a result, the published algorithms are still not accurate enough.

MLP-based models These methods use multi-layer perceptron (MLP) to predict the type of each residue. The MLP outputs the probability of 20 amino acids for each residue, and the input feature construction is the main difference between various methods. SPIN (Li et al., 2014) integrates torsion angles (ϕ and ψ), fragment-derived sequence profiles and structure-derived energy profiles to predict protein sequences. SPIN2 (O’Connell et al., 2018) adds backbone angles (θ and τ), local concat number and neighborhood distance to improve the accuracy from 30%

to 34%. (Wang et al., 2018) uses backbone dihedrals (ϕ , ψ and ω), solvent accessible surface area of backbone atoms (C_α , N , C , and O), secondary structure types (helix, sheet, loop), $C_\alpha - C_\alpha$ distance and unit direction vectors of $C_\alpha - C_\alpha$, $C_\alpha - N$ and $C_\alpha - C$, which achieves 33.0% accuracy on 50 test proteins. The MLP methods have a high inference speed, but their accuracy is relatively low due to the partial considering of structural information. The complex feature engineering requires multiple databases and computational tools, limiting the widespread usage.

CNN-based models CNN methods extract protein features directly from the 3D structure, which can be further classified as 2D CNN-based and 3D CNN-based, with the latter achieving better results. The 2D CNN-based SPROF (Chen et al., 2019) extracts structural features from the distance matrix, and improves the accuracy to 39.8%. In contrast, 3D CNN-based methods extract residue features from the atom distribution in a three-dimensional grid box. For each residue, the atomic density distribution is computed after being translated and rotated to a standard position so that the model can learn translation and rotation invariant features. ProDCoNN (Zhang et al., 2020a) designs a nine-layer 3D CNN to predict the corresponding residues at each position, which uses multi-scale convolution kernels and achieves 42.2% accuracy. DenseCPD (Qi & Zhang, 2020) further uses the DensetNet architecture (Huang et al., 2017) to boost the accuracy to 55.53%. Although 3DCNN-based models improve accuracy, their inference is slow, probably because they require separate pre-processing and prediction for each residue. In addition, none of the above 3D CNN models are open source.

Graph-based models Graph methods represent the 3D structure as a k -NN graph, then use graph neural networks (Defferrard et al., 2016; Kipf & Welling, 2016; Veličković et al., 2017; Zhou et al., 2020; Zhang et al., 2020b) to extract residue features while considering structural constraints. The protein graph encodes the residue information in node vectors and constructs edges and edge features between neighboring residues. GraphTrans (Ingraham et al., 2019) achieves 36.4% accuracy using graph attention and autoregression generation strategies. GVP (Jing et al., 2020) increases the accuracy to 40.2% by proposing the geometric vector perceptron, which learns both scalar and vector features in an equivariant and invariant manner with respect to rotations and reflections. Another related work is Protein-Solver (Strokach et al., 2020), but it was mainly developed for scenarios where partial sequences are known and does not report results on standard datasets. Firstly, since both GraphTrans and GVP use rotated, translation-invariant features, there is no need to rotate each residue separately as in CNN, thus improving the training efficiency. However, during testing, GraphTrans and GVP use an autoregressive mechanism to generate residuals one by one rather than in

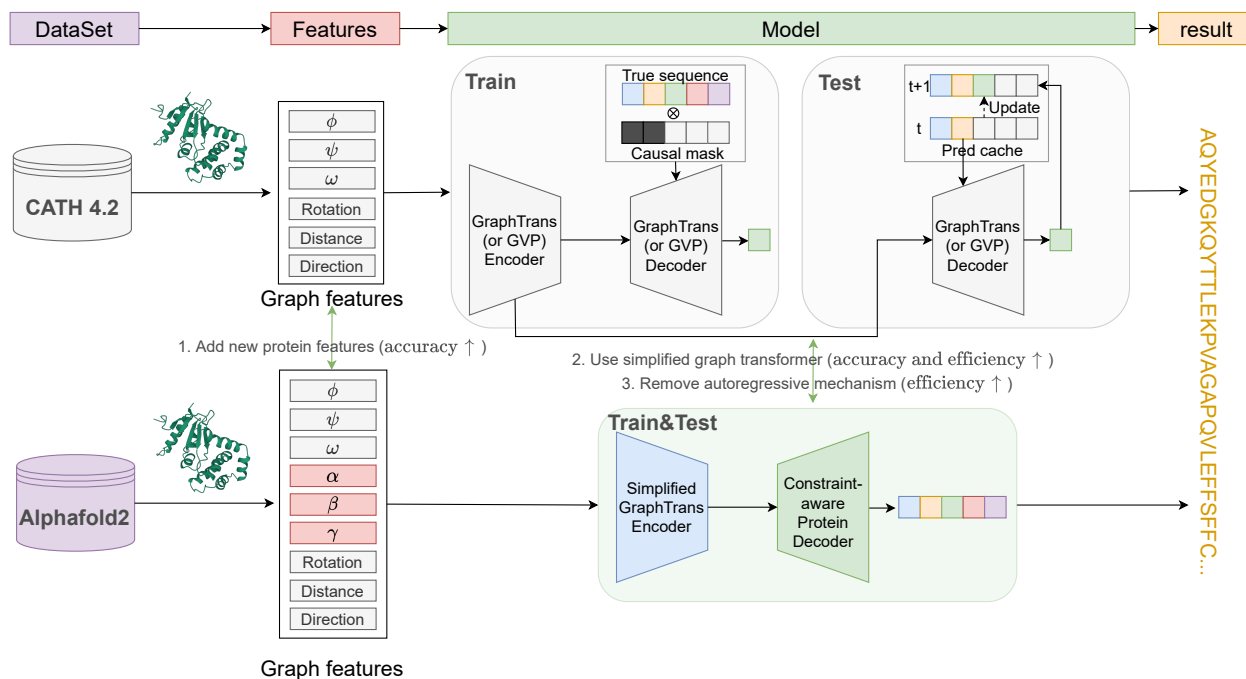


Figure 1. Overview of ADesign. Compared with GraphTrans, StructGNN (Ingraham et al., 2019) and GVP (Jing et al., 2020), we add new protein features, simplify the graph transformer, and propose a confidence-aware protein decoder to improve accuracy.

parallel, which weakens their advantage in inference speed. Secondly, the well-exploited structural information helps GNN obtain higher accuracy than MLPs. In summary, GNN can achieve a good balance between efficiency and accuracy.

Challenges There are several challenges that hinder the research progress: (C1) As shown in Table. 1, different methods may use inconsistent datasets, which will affect the researcher’s judgment of the model’s ability. (C2) The reported prediction accuracy is still low, i.e., none of the existing models exceeds 50% accuracy except DenseCPD. (C3) The most accurate CNN model has poor efficiency, e.g., DenseCPD takes 7 minutes to predict a 120-length protein on their server. By the way, (C4) the accessibility is poor. Because most protein design models are not open source, subsequent studies become relatively difficult.

	Method	N_{train}	N_{test}	Acc	Code
MLP	SPIN	1,532	500	30%	no
	SPIN2	1,532	500	34%	no
	Wang’s model	10,173	50	33%	no
CNN	SPOF	7,134	922	39.8%	PyTorch
	ProDCoNN	17,044	4,027	46.5%	no
	DenseCPD	$\leq 10,727$	500	55.53%	no
GNN	GraphTrans	18,024	1,120	36.4%	PyTorch
	GVP	18,024	1,120	40.2%	PyTorch

Table 1. Statistics of structure-based protein design methods. N_{train} and N_{test} is the number of training set and testing set. Acc indicates the sequence recovery score on TS50.

For C1, we establish the *new AlphaDesign benchmark* in section. 4. For C2 and C3, we propose *ADesign method to achieve SOTA accuracy and efficiency*, seeing section. 3 and section. 4. As to C4, our model will be open source to accelerate research progress.

3. Methods

3.1. Overview

As shown in Fig. 1, we present the overall framework of ADesign, where the methodological innovations include:

- **Expressive features:** We add new proteins angles (α, β, γ) to steadily improve the model accuracy.
- **Better graph encoder:** We use the simplified graph transformer (SGT) to extract more expressive representations, where the multi-head attention weights are learned through MLP without multiplying Q and K .
- **Fast sequence decoder:** We propose **constraint-aware protein decoder (CPD)** to replace the autoregressive generator, which can predict residues in parallel and simplify the algorithm.

With these changes, the proposed ADesign is more accurate, simple, and efficient than previous approaches and, therefore, more attractive as a future baseline model.

3.2. Graph encoder

The protein structure can be viewed as a special 3D point cloud in which the order of residues is known. For ordinary 3D points, there are two way to get rotation and translation invariant features: Using special network architecture (Fuchs et al., 2020; Satorras et al., 2021; Jing et al., 2020; Shuaibi et al., 2021) that taking 3D points as input or using handicraft invariant features. For proteins, general 3D point cloud approaches cannot consider its particularity, including the regular structure and order of amino acids. Therefore, we prefer learning from the hand-designed, invariant, and protein-specific features. So, which handcrafted invariant features should be constructed? And how to learn expressive representations from these features?

Graph We represent the protein as a k -NN graph derived from residues to consider the 3D dependencies, where k defaults to 30. The protein graph $\mathcal{G}(A, X, E)$ consists of the adjacency matrix $A \in \{0, 1\}^{n, n}$, node features $X \in \mathbb{R}^{n, 12}$, and edge features $E \in \mathbb{R}^{m, 23}$. Note that n and m are the numbers of nodes and edges, and we create these features by the regular structure, order, and coordinate of residues.

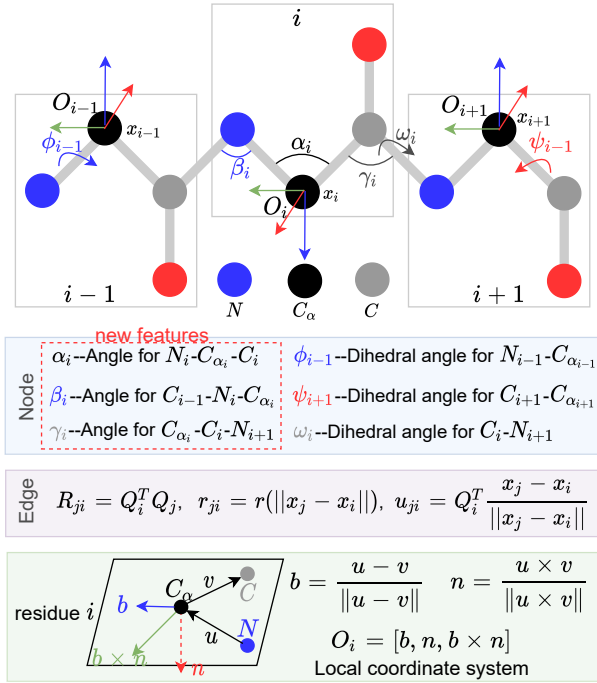


Figure 2. Angles of the protein backbone.

Node features As shown in Fig. 2, we consider two kinds of angles as node features, i.e., the angles α, β, γ formed by adjacent edges and the dihedral angles ϕ, ψ, ω formed by adjacent surfaces, where α, β, γ are new features we introduced. For better understanding dihedral angles, it is worth stating that ϕ_{i-1} is the angle between plane $C_{i-2} - N_{i-1} - C_{\alpha_{i-1}}$ and $N_{i-1} - C_{\alpha_{i-1}} - C_{i-1}$, whose intersection

is $N_{i-1} - C_{\alpha_{i-1}}$. Finally, there are 12 node features derived from $\{\sin, \cos\} \times \{\alpha, \beta, \gamma, \phi, \psi, \omega\}$.

Edge features For edge $j \rightarrow i$, we use relative rotation R_{ji} , distance r_{ji} , and relative orientation u_{ji} as edge features, seeing Fig. 2. At the i -th residue’s alpha carbon, we establish a local coordinate system $O_i = (b_i, n_i, b_i \times n_i)$. The relative rotation between O_i and O_j is $R_{ji} = Q_i^T Q_j$ can be represented by an quaternion $q(R_{ji})$. We use radial basis $r(\cdot)$ to encode the distance between C_{α_i} and C_{α_j} . The relative direction of C_{α_j} respective to C_{α_i} is calculated by $u_{ji} = Q_i^T \frac{x_j - x_i}{\|x_j - x_i\|}$. In summary, there are 23 edge features: 4(quaternion) + 16(radial basis) + 3(relative direction).

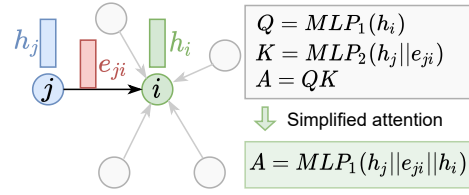


Figure 3. Simplified graph transformer.

Simplified graph transformer Denote h_i^l and e_{ji}^l as the output feature vectors of node i and edge $j \rightarrow i$ in layer l . We use MLP to project input node and edge features into d -dimensional space, thus $h_i^0 \in \mathbb{R}^d$ and $e_{ji}^0 \in \mathbb{R}^d$. When considering the attention mechanisms centered in node i , the attention weight a_{ji} at the $l + 1$ layer is calculated by:

$$\begin{cases} w_{ji} = MLP_1(h_j^l || e_{ji}^l || h_i^l) \\ a_{ji} = \frac{\exp w_{ji}}{\sum_{k \in \mathcal{N}_i} \exp w_{ki}} \end{cases} \quad (2)$$

where \mathcal{N}_i is the neighborhood system of node i and $||$ means the concatenation operation. Here, we simplify GraphTrans (Ingraham et al., 2019) by using a single MLP to learn multi-headed attention weights instead of using separate MLPs to learn Q and K , seeing Fig. 3. The updated h_i^{l+1} is:

$$\begin{cases} v_j = MLP_2(e_{ji}^l || h_j^l) \\ h_i^{l+1} = \sum_{j \in \mathcal{N}_i} a_{ji} v_j \end{cases} \quad (3)$$

By stacking multiple simplified graph transformer (SGT) layers, we can obtain expressive protein representations, which consider both 3D structural constraints by GNN and the 1D information of the manually designed input features.

3.3. Sequence decoder

To generate more accurate protein sequences, previous researches (Ingraham et al., 2019; Jing et al., 2020) prefer the autoregressive mechanism. However, this technique also significantly slows down the inference process because the residuals must be predicted one by one. *Can we parallelize the predictor while maintaining the accuracy?*

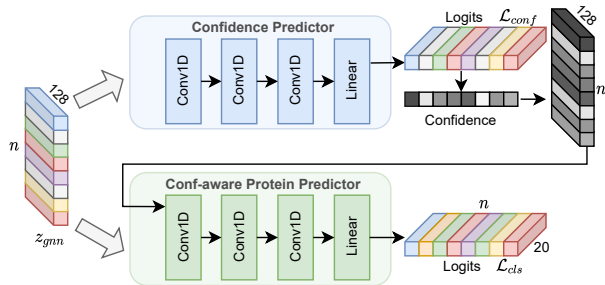


Figure 4. CPD: The confidence-aware protein decoder. We use two 1D CNN networks to learn confidence scores and make final predictions based on the input graph node features.

Context-aware Previously, we have considered the 3D constraints through graph network but ignored 1D inductive bias in the neural model. Now, we use 1D CNNs to capture the local sequential dependencies based on the 3D context-aware graph node features. As shown in Fig. 4, the input features are $Z_{gmn} = \{z_1, z_2, \dots, z_N\}$, where z_i is the feature vector of node i extracted by previous GNN. The convolution kernel can be viewed as the sliding window.

Confidence-aware Given the 3D structure $\mathcal{X} = \{x_i : 1 \leq i \leq N\}$ and protein sequence $\mathcal{S} = \{s_i : 1 \leq i \leq N\}$, the vanilla autoregressive prediction indicates $p(\mathcal{S}|\mathcal{X}) = \prod_i p(s_i|\mathcal{X}, s_{<i})$, where residues must be predicted one-by-one. We replace autoregressive connections with parallelly estimated confidence score c , written as

$$\begin{cases} c = f(\text{Conf}(\mathcal{X})) \\ p(\mathcal{S}|\mathcal{X}) = \prod_i p(s_i|\mathcal{X}, x_i, c_i) \end{cases} \quad (4)$$

where c is the predictive confidence estimated by an auxiliary classifier $\text{Conf}(\cdot)$. The confidence score contains knowledge captured by the previous prediction and plays a similar role to the autoregressive connections. Let $M \in \mathbb{R}^{n,1}$ and $m \in \mathbb{R}^{n,1}$ as Conf 's first and secondary largest logits vector of n residues, the confidence score is defined as:

$$c = \lfloor \frac{M}{m} \rfloor. \quad (5)$$

We encode the confidence score as learnable embeddings $\mathcal{C} \in \mathbb{R}^{n,128}$, concatenate them with graph features, and feed these features into another classifier to get final predictions. Note that all classifiers for estimating confidence and final predictions use the same CE loss:

$$\mathcal{L} = - \sum_i \sum_{1 \leq j \leq 20} \mathbb{1}_{\{j\}}(y_i) \log(p_{i,j}). \quad (6)$$

where $p_{i,j}$ is the predicted probability that residue i 's type is j , y_i is the true label and $\mathbb{1}_{\{j\}}(\cdot)$ is an indicator function.

4. Experiments

We conduct systematical experiments to establish the new AlphaDesign benchmark and evaluate the proposed ADesign method. Specifically, we aim to answer:

- **Q1:** What is the difference between the new benchmark and the old one?
- **Q2:** Can ADesign achieve SOTA accuracy on the new benchmark?
- **Q3:** Does ADesign efficient enough in both the training and testing phase?
- **Q4:** What is the secret to achieving SOTA performance? What really matters?

4.1. Benchmark comparison (Q1)

Metric Following (Li et al., 2014; O'Connell et al., 2018; Wang et al., 2018; Ingraham et al., 2019; Jing et al., 2020), we use sequence recovery to evaluate different protein design methods. Compared with other metrics, such as perplexity, recovery is more intuitive and clear, and its value is equal to the average accuracy of predicted amino acids in a single protein sequence. By default, we report the median recovery score across the entire test set.

Previous benchmark In Table. 2, we show the old benchmark collected from previous studies, including MLP (Li et al., 2014; O'Connell et al., 2018; Wang et al., 2018), CNN (Chen et al., 2019; Zhang et al., 2020a; Qi & Zhang, 2020; Huang et al., 2017) and GNN (Ingraham et al., 2019; Jing et al., 2020; Strokach et al., 2020) models. Most approaches report results on the common test set TS50, consisting of 50 small proteins between 60 and 200 in length (Li et al., 2014). SOTA graph models, e.g., GraphTrans, StructGNN (Ingraham et al., 2019), and GVP (Jing et al., 2020), are also compared on a CATH test set with 1120 chains.

Weakness While the TS50 significantly contributes to establishing the benchmark, we have two concerns: (1) such a small number of proteins does not cover the vast protein space and is more likely to lead to biased tests, and (2) there are no canonical training and validation sets, which means that different methods may use various training sets. Regarding the first concern, TS50 provides limited experimental evidence for protein design, and we need more test data to know how the algorithm performs in more general cases. As to the second concern, if the training data are inconsistent, how can we convince researchers that the performance improvement comes from methods rather than data? Especially when the test set is small, it is much easier to construct the training set to fit the test set manually.

	N_{train}	CATH	TS50
GVP (Jing et al., 2020)	18,024	40.2	44.9
StructGNN (Ingraham et al., 2019)	18,024	37.3	–
GraphTrans (Ingraham et al., 2019)	18,024	36.4	–
DesnseCPD (Qi & Zhang, 2020)	$\leq 10,727$	–	50.7
ProDCoNN (Zhang et al., 2020a)	17,044	–	40.7
SBROF (Chen et al., 2019)	7,134	–	39.2
SPIN2 (O’Connell et al., 2018)	1,532	–	33.6
Wang’s model (Wang et al., 2018)	10,179	–	33.0
ProteinSolver (Strokach et al., 2020)	18,024	–	30.8
SPIN (Li et al., 2014)	1,532	–	30.3
Rosetta (Leaver-Fay et al., 2011)	–	–	30.0

Table 2. Old benchmark. We show recovery scores of various methods on CATH and TS50 test set, where the number of training data N_{train} may vary in different methods.

New dataset We use the AlphaFold Protein Structure Database ² (Varadi et al., 2021) to benchmark graph-based protein design methods. As shown in Table. 3, there are over 360,000 predicted structures by AlphaFold2 (Jumper et al., 2021) across 21 model-organism proteomes. This dataset has several advantages:

- Species-aware: This dataset provides well-organized proteomic data for different species, which is helpful to develop specialized models for each species.
- More structures: This dataset provides more than 360,000 structures, while previous Protein Data Bank (PDB) (Burley et al., 2021) holds just over 180,000 structures for over 55,000 distinct proteins.
- High quality: The median predictive score of AlphaFold2 reaches 92.4%, comparable to experimental techniques (Callaway, 2020). In 2020, the CASP14 benchmark has recognized AlphaFold2 as a solution to the protein-folding problem (Pereira et al., 2021).
- Missing value: There are no missing values in protein structures provided by AlphaFold DB.

Novel settings We extend the experimental setups to length-free and species-aware compared to previous studies (Ingraham et al., 2019; Jing et al., 2020) that use length-limited proteins and do not discriminate species. Length-free means that the protein length may be arbitrary to generalize the model to broader situations; otherwise, the protein must be between 30 and 500 in length. Species-aware indicates that we develop a specific model for each organism’s proteome to learn domain-specific knowledge; otherwise, we use the joint proteomic data to train one model for all species. In summary, there are four settings:

- SL: Separate proteomic data + Limited length.
- SF: Separate proteomic data + Free length.

²<https://alphafold.ebi.ac.uk>

ID	Name	Structures	≤ 30	(30, 500]	[500, 1000]	> 1000
1	DANRE	24,664	27	15,460	6,573	2,604
2	CANAL	5,974	0	3,656	1,874	444
3	MOUSE	21,615	55	13,767	5,668	2,125
4	ECOLI	4,363	63	3,719	526	55
5	DROME	13,458	28	8,509	3,563	1,358
6	METJA	1,773	0	1,605	144	24
7	PLAF7	5,187	1	2,832	1,313	1,041
8	MYCTU	3,988	4	3,365	536	83
9	CAEEL	19,694	52	15,073	3,592	977
10	DICDI	12,622	3	7,663	3,367	1,589
11	TRYCC	19,036	6	12,622	5,007	1,401
12	YEAST	6,040	24	3,789	1,715	512
13	SCHPO	5,128	5	3,385	1,386	352
14	RAT	21,272	12	13,884	5,370	2,006
15	HUMAN	23,391	49	12,399	5,653	5,290
16	ARATH	27,434	42	19,885	6,389	1,118
17	MAIZE	39,299	83	29,145	8,360	1,711
18	LEIIN	7,924	0	4,276	2,505	1,143
19	STAA8	2,888	22	2,567	267	32
20	SOYBN	55,799	17	41,048	12,353	2,381
21	ORYSJ	43,649	78	35,987	6,738	846
	Sum	365,198	571	254,636	82,899	27,092

Table 3. AlphaFold DB: we show the total number of proteins N_{all} , and the number of proteins whose length within (0, 30], (30, 500], (500, 1000] and (1000, $+\infty$]. The statistics of all proteomic data are also presented.

- JL: Joint proteomic data + Limited length.
- JF: Joint proteomic data + Free length.

Denote the total amount of structures as N_{all} , and the i -th species has N_i structures, we have $N_{all} = \sum_{i=1}^{21} N_i$. As shown in Table. 3, if the length is limited, $N_{all} = 254,636$; otherwise, $N_{all} = 365,198$. When we use separate proteomic data, we develop 21 models based on datasets with N_1, N_2, \dots, N_{21} structures; otherwise, we train one model using the joint dataset with N_{all} structures for all species.

4.2. AlphaDesign benchmark (Q2)

Data split Under the SL and SF setting, for the i -th specie, we randomly choose $90\%N_i$ samples for training, 100 for validation, and $(10\%N_i - 100)$ for testing. Correspondingly, in the JL and JF setting, we combine the these sets of all species, resulting in $\sum_{i=1}^{21} 90\%N_i$ proteins for training, 21×100 for validation, and $(\sum_{i=1}^{21} 10\%N_i - 2100)$ for testing. In addition, it should be noted that for each species, its training sets under SL and SF settings are unrelated, as are the validation sets and test sets. Last but not least, under the same setting, all methods use the same training, validation, and testing sets.

SL and JL settings In SL and JL settings, the structure length must be between 30 and 500. By default, we use Adam optimizer, OneCycleLR scheduler to train all models up to 100 epochs with earllystop patience 20. Besides, we set the batch_size of GraphTrans, StructGNN, and ADesign as

16 and the max_node of GVP as 2000. Note that max_node represents the maximum number of residuals per batch. Under the SL setting, the learning rate is 0.01. Under the JL setting, we reduce the learning rate and epochs to 0.001 and 50, and increase batch_size to 32. Please refer to Table. 7 (in the appendix) for a clearer understanding of the model parameter settings.

SL and JL results We present the SL and JL benchmarks in Table. 4, and conclude that the order of model accuracy from high to low is ADesign > GVP > SGNN > GTrans under the SL setting. It is worth mentioning that ADesign exceeds previous methods by 8% accuracy on average. We also observe that ADesign (JL) is less accurate than ADesign (SL), possibly because the latter is more likely to learn species-related knowledge.

	GTrans	SGNN	GVP	Our(SL)	Gain	Our(JL)
DANRE	51.8	52.5	<u>53.2</u>	63.5	+10.3	48.2
CANAL	45.2	46.2	<u>48.5</u>	55.1	+6.6	48.9
MOUSE	52.5	53.0	<u>55.0</u>	64.7	+9.7	45.7
ECOLI	50.0	49.4	<u>51.9</u>	52.7	+0.8	50.8
DROME	49.6	49.2	<u>51.2</u>	60.3	+9.1	47.5
METJA	48.9	49.6	<u>50.9</u>	53.4	+2.5	48.7
PLAF7	45.0	45.9	<u>48.6</u>	54.3	+5.7	37.3
MYCTU	53.4	53.7	<u>56.9</u>	61.8	+4.9	57.8
CAEEL	51.4	52.3	<u>54.1</u>	63.9	+9.8	44.1
DICDI	49.7	50.2	<u>52.0</u>	61.4	+9.4	41.6
TRYCC	52.4	52.5	<u>53.2</u>	65.7	+12.5	47.9
YEAST	44.6	44.6	<u>48.9</u>	53.9	+5.0	47.2
SCHPO	45.8	45.1	<u>47.8</u>	53.5	+5.7	50.4
RAT	52.2	52.6	<u>53.8</u>	64.2	+10.4	46.1
HUMAN	52.3	52.3	<u>53.8</u>	63.5	+9.7	48.2
ARATH	52.3	53.2	<u>54.3</u>	65.1	+10.8	47.5
MAIZE	54.1	54.9	<u>56.0</u>	67.9	+11.9	48.3
LEIIN	47.6	48.8	<u>50.7</u>	57.5	+6.8	54.6
STAA8	46.3	46.3	<u>48.7</u>	52.4	+3.7	44.6
SOYBN	53.1	54.1	<u>55.6</u>	67.2	+11.6	45.1
ORYSJ	55.2	56.3	<u>58.0</u>	69.5	+11.5	44.9
Average	50.2	50.6	<u>52.5</u>	60.5	+8.0	47.4

Table 4. SL and JL benchmarks. We report the median recovery scores across the test set. Due to space constraints, we introduce abbreviations such as GTrans for GraphTrans and SGNN for Struct GNN. ADesign not only compares with baselines in the SL setting, but also provides results under the JL setting. We highlight the best results in bold and underline the sub-optimum ones.

SF and JF settings In SF and JF settings, the protein length can be arbitrary. Under the SF setting, all experimental details remain consistent with the SL setup, except for the batch_size of baseline models. Since the maximum structural length can be up to 2700 in AlphaFold DB, we change GVP’s max_node parameter to 3000 to make it applicable to all data. In addition, GraphTrans and StructGNN take more GPU memories because they must pad data according to the longest chain in each batch, and we adjust their batch_size as 8 to avoid memory overflow. Under the JF setting, we

also reduce the learning rate and epochs to 0.001 and 50, and increase batch_size to 32.

SF and JF results We present the SL and JL benchmarks in Table. 5 and observe that our ADesign is still the best model, while the sub-optimum results are achieved by SGNN rather than GVP. This probably because GVP is sensitive to the max_node parameter, while other methods are robust to batch_size. Besides, the increase in the amount of training data further improves the model, i.e., the average accuracy of ADesign (SF) is 62.3% while that of ADesign (SL) is 60.5%. As a result, ADesign (SF) outperforms baselines by 9.4%. Finally, we provide results of ADesign (JF) for broader comparisons.

	GTrans	SGNN	GVP	Our(SF)	Gain	Our(JF)
DANRE	51.9	<u>54.7</u>	44.2	64.2	+9.5	51.9
CANAL	48.7	<u>51.3</u>	41.3	58.4	+7.1	53.9
MOUSE	53.1	<u>55.6</u>	44.8	65.6	+10.0	50.7
ECOLI	<u>50.6</u>	50.0	45.3	56.8	+6.2	56.0
DROME	50.2	<u>52.3</u>	43.0	62.4	+10.1	50.6
METJA	49.8	47.9	44.0	53.9	+4.1	51.1
PLAF7	49.6	<u>50.6</u>	41.5	58.4	+7.8	42.5
MYCTU	<u>53.9</u>	53.2	48.5	61.9	+8.0	59.5
CAEEL	51.8	<u>53.6</u>	43.6	62.6	+9.0	45.9
DICDI	52.8	<u>54.9</u>	44.9	64.5	+9.6	47.1
TRYCC	53.1	<u>54.9</u>	45.0	65.9	+11.0	51.5
YEAST	47.2	<u>47.3</u>	40.5	57.0	+9.7	51.1
SCHPO	47.5	<u>50.0</u>	41.6	55.7	+5.7	53.7
RAT	53.2	<u>55.2</u>	44.2	66.4	+11.2	49.5
HUMAN	52.6	<u>54.3</u>	44.3	65.1	+10.8	50.6
ARATH	53.6	<u>55.0</u>	44.6	64.9	+9.9	50.8
MAIZE	54.7	<u>56.5</u>	47.1	68.7	+12.2	52.0
LEIIN	50.9	<u>52.2</u>	44.3	63.3	+11.1	56.9
STAA8	<u>46.6</u>	46.3	42.5	52.7	+6.1	50.5
SOYBN	54.0	<u>54.8</u>	45.6	70.3	+15.5	48.7
ORYSJ	55.6	<u>57.3</u>	46.7	69.1	+11.8	44.1
Average	51.5	<u>52.8</u>	41.2	62.3	9.4	50.9

Table 5. SF and JF benchmarks. We highlight the best recovery scores in bold and underline the sub-optimum ones.

Summary Experiments on both SL and SF settings show that ADesign consistently outperforms previous baseline methods and achieves new SOTA accuracy. This improvement is stable and significant, with an average improvement of over 8%. If we extend SL and SF to JL and JF, the performance will be degraded, possibly because it is easier to learn species-related knowledge through separated proteomic datasets. However, it is also possible that the insufficient model parameters cause performance degradation. Developing a stronger large model applied to all species could be a future direction.

4.3. Efficiency comparison (Q3)

A good algorithm should have high accuracy and excellent computational efficiency. Although previous experiments have demonstrated the accuracy advantage of ADesign, we

don’t know whether it is computationally faster than baselines. Now, we study the training and testing speed of different models on multi-scale datasets.

Setting In both SL and SF settings, we use training data of 5K, 10K, 15K, 20K, and equipped with test samples of 0.5K, 1K, 1.5K, and 2K, respectively, to evaluate the model efficiency. During training, the batch_size of GraphTrans, StructGNN and ADesign is 8, and the max_node parameter of GVP is 3000. During testing, each protein is separately fed into the model for prediction, i.e. batch_size =1.

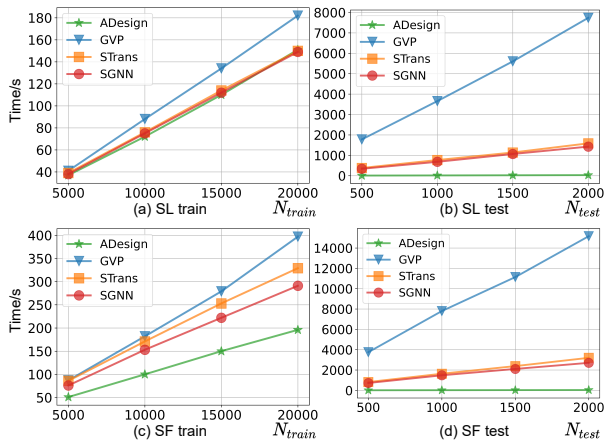


Figure 5. Speed in SL and SF settings. We show the training time (per epoch) and testing time of various methods, where N_{train} and N_{test} are the data amount of training set and testing set.

Speed In Fig. 5, we show the running time of various models. In the SL setting, the order of training efficiency from high to low is ADesign \approx StructGNN>GraphTrans>GVP, seeing Fig. 5 (a). During testing, ADesign runs at least 40 times faster than other methods, e.g., SGNN takes 1,430s to evaluate 2,000 proteins while ADesign takes only 30 seconds. Under the SF setting, ADesign has the best runtime efficiency at all stages. In contrast, SGNN and GTrans seem to be slower than before, because they need to pad inputs according to the longest structure in each batch, and the longest structure in SL setting is longer than that in SF setting. By the same reasoning, increasing the batch_size gives ADesign a more significant speedup than SGNN and GTrans at all settings. According to our understanding, the reasons behind the excellent efficiency of ADesign include: (1) We use a simplified graph attention mechanism to speed up feature extraction; (2) We use CPD instead of complex autoregressive decoders to parallelize prediction.

4.4. Ablation study (Q4)

While ADesign has shown great performance, we are more interested in where the improvements come from. As we have mentioned before, we add new protein features, simplify the graph transformer, and propose a confidence-aware

protein decoder to improve accuracy. Then, how much gain can be obtained from each change? Are there redundant changes that are useless for performance improvement?

Setting We conduct ablation experiments on ADesign under the SL setting. Specifically, we may replace the simplified attention module with original GraphTrans (w/o Enc), replace the CPD module with vanilla MLP (w/o Dec), or remove the newly introduced angle features (w/o new feat). Except for model differences, all experimental settings keep the same with previous SL settings.

Results and analysis The ablation results are shown in Table. 6. Based on the ablation study and section 4.3, we conclude that: (1) The three changes recommended in this paper can bring steady and significant improvements. (2) As to accuracy, the most crucial part is the newly added features, followed by the simplified graph encoder, and finally, the sequence decoder. (3) The confidence-aware protein decoder dramatically improves the evaluation speed, as well as brings considerable accuracy gains.

	ADesign	w/o Enc	w/o Dec	w/o new feat
DANRE	63.5	59.2	60.6	54.8
CANAL	55.1	49.6	52.7	42.3
MOUSE	64.7	58.4	60.8	55.3
ECOLI	52.7	42.5	48.4	41.9
DROME	60.3	55.1	55.8	49.7
METJA	53.4	44.0	53.2	44.1
PLAF7	54.3	47.5	53.4	42.6
MYCTU	61.8	55.6	57.4	50.0
CAEEL	63.9	59.3	60.2	55.5
DICDI	61.4	55.2	58.1	50.7
TRYCC	65.7	60.6	61.2	56.8
YEAST	53.9	48.6	52.5	42.3
SCHPO	53.5	48.5	52.3	43.2
RAT	64.2	58.9	61.1	54.7
HUMAN	63.5	58.6	59.9	53.3
ARATH	65.1	61.1	62.0	55.8
MAIZE	67.9	64.7	63.4	61.8
LEIIN	57.5	52.3	55.8	48.0
STAA8	52.4	43.3	52.2	43.2
SOYBN	67.2	64.0	64.8	57.9
ORYSJ	69.5	66.1	66.7	59.4
Average	60.5	54.9	57.7	50.6

Table 6. Ablation study under the SL setting.

5. Conclusion

This paper establishes a new benchmark—AlphaDesign, and proposes a new ADesign method for AI-guided protein design. By introducing new protein features, simplifying the graph transformer, and proposing a confidence-aware protein decoder, ADesign achieves state-of-the-art accuracy and efficiency. We hope this work will help standardize comparisons and provide inspiration for subsequent researches.

References

- Burley, S. K., Bhikadiya, C., Bi, C., Bittrich, S., Chen, L., Crichlow, G. V., Christie, C. H., Dalenberg, K., Di Costanzo, L., Duarte, J. M., et al. Rcsb protein data bank: powerful new tools for exploring 3d structures of biological macromolecules for basic and applied research and education in fundamental biology, biomedicine, biotechnology, bioengineering and energy sciences. *Nucleic acids research*, 49(D1):D437–D451, 2021.
- Callaway, E. 'it will change everything': Deepmind's ai makes gigantic leap in solving protein structures. *Nature*, pp. 203–204, 2020.
- Chen, S., Sun, Z., Lin, L., Liu, Z., Liu, X., Chong, Y., Lu, Y., Zhao, H., and Yang, Y. To improve protein sequence profile prediction through image captioning on pairwise residue distance map. *Journal of chemical information and modeling*, 60(1):391–399, 2019.
- Defferrard, M., Bresson, X., and Vandergheynst, P. Convolutional neural networks on graphs with fast localized spectral filtering. *Advances in neural information processing systems*, 29:3844–3852, 2016.
- Fuchs, F. B., Worrall, D. E., Fischer, V., and Welling, M. Se (3)-transformers: 3d roto-translation equivariant attention networks. *arXiv preprint arXiv:2006.10503*, 2020.
- Huang, G., Liu, Z., Van Der Maaten, L., and Weinberger, K. Q. Densely connected convolutional networks. In *Proceedings of the IEEE conference on computer vision and pattern recognition*, pp. 4700–4708, 2017.
- Huo, Y.-X., Cho, K. M., Rivera, J. G. L., Monte, E., Shen, C. R., Yan, Y., and Liao, J. C. Conversion of proteins into biofuels by engineering nitrogen flux. *Nature biotechnology*, 29(4):346–351, 2011.
- Ingraham, J., Garg, V. K., Barzilay, R., and Jaakkola, T. Generative models for graph-based protein design. 2019.
- Jing, B., Eismann, S., Suriana, P., Townshend, R. J., and Dror, R. Learning from protein structure with geometric vector perceptrons. *arXiv preprint arXiv:2009.01411*, 2020.
- Jumper, J., Evans, R., Pritzel, A., Green, T., Figurnov, M., Ronneberger, O., Tunyasuvunakool, K., Bates, R., Židek, A., Potapenko, A., et al. Highly accurate protein structure prediction with alphafold. *Nature*, 596(7873):583–589, 2021.
- Kipf, T. N. and Welling, M. Semi-supervised classification with graph convolutional networks. *arXiv preprint arXiv:1609.02907*, 2016.
- Leaver-Fay, A., Tyka, M., Lewis, S. M., Lange, O. F., Thompson, J., Jacak, R., Kaufman, K. W., Renfrew, P. D., Smith, C. A., Sheffler, W., et al. Rosetta3: an object-oriented software suite for the simulation and design of macromolecules. *Methods in enzymology*, 487:545–574, 2011.
- Li, Z., Yang, Y., Faraggi, E., Zhan, J., and Zhou, Y. Direct prediction of profiles of sequences compatible with a protein structure by neural networks with fragment-based local and energy-based nonlocal profiles. *Proteins: Structure, Function, and Bioinformatics*, 82(10):2565–2573, 2014.
- O'Connell, J., Li, Z., Hanson, J., Heffernan, R., Lyons, J., Paliwal, K., Dehzangi, A., Yang, Y., and Zhou, Y. Spin2: Predicting sequence profiles from protein structures using deep neural networks. *Proteins: Structure, Function, and Bioinformatics*, 86(6):629–633, 2018.
- Pabo, C. Molecular technology: designing proteins and peptides. *Nature*, 301(5897):200–200, 1983.
- Pearson, W. R. and Sierk, M. L. The limits of protein sequence comparison? *Current opinion in structural biology*, 15(3):254–260, 2005.
- Pereira, J., Simpkin, A. J., Hartmann, M. D., Rigden, D. J., Keegan, R. M., and Lupas, A. N. High-accuracy protein structure prediction in casp14. *Proteins: Structure, Function, and Bioinformatics*, 89(12):1687–1699, 2021.
- Qi, Y. and Zhang, J. Z. Denscpd: improving the accuracy of neural-network-based computational protein sequence design with densenet. *Journal of chemical information and modeling*, 60(3):1245–1252, 2020.
- Satorras, V. G., Hoogeboom, E., and Welling, M. E (n) equivariant graph neural networks. *arXiv preprint arXiv:2102.09844*, 2021.
- Shuaibi, M., Kolluru, A., Das, A., Grover, A., Sriram, A., Ulissi, Z., and Zitnick, C. L. Rotation invariant graph neural networks using spin convolutions. *arXiv preprint arXiv:2106.09575*, 2021.
- Strokach, A., Becerra, D., Corbi-Verge, C., Perez-Riba, A., and Kim, P. M. Fast and flexible protein design using deep graph neural networks. *Cell Systems*, 11(4):402–411, 2020.
- Varadi, M., Anyango, S., Deshpande, M., Nair, S., Natassia, C., Yordanova, G., Yuan, D., Stroe, O., Wood, G., Laydon, A., et al. Alphafold protein structure database: Massively expanding the structural coverage of protein-sequence space with high-accuracy models. *Nucleic acids research*, 2021.

- Veličković, P., Cucurull, G., Casanova, A., Romero, A., Lio, P., and Bengio, Y. Graph attention networks. arXiv preprint arXiv:1710.10903, 2017.
- Wang, J., Cao, H., Zhang, J. Z., and Qi, Y. Computational protein design with deep learning neural networks. Scientific reports, 8(1):1–9, 2018.
- Williams, S. A., Kivimaki, M., Langenberg, C., Hingorani, A. D., Casas, J., Bouchard, C., Jonasson, C., Sarzynski, M. A., Shipley, M. J., Alexander, L., et al. Plasma protein patterns as comprehensive indicators of health. Nature medicine, 25(12):1851–1857, 2019.
- Zhang, Y., Chen, Y., Wang, C., Lo, C.-C., Liu, X., Wu, W., and Zhang, J. Prodcnn: Protein design using a convolutional neural network. Proteins: Structure, Function, and Bioinformatics, 88(7):819–829, 2020a.
- Zhang, Z., Cui, P., and Zhu, W. Deep learning on graphs: A survey. IEEE Transactions on Knowledge and Data Engineering, 2020b.
- Zhou, J., Cui, G., Hu, S., Zhang, Z., Yang, C., Liu, Z., Wang, L., Li, C., and Sun, M. Graph neural networks: A review of methods and applications. AI Open, 1:57–81, 2020.

A. Appendix

A.1. Hyper-parameters

Setting	Seperate data	Limited length	N_{train}	N_{val}	N_{test}	batch_size (GraphTrans)	max_node (GVP)	batch_size (ADesign)	lr	epoch
SL	yes	yes	$0.9N_i$	100	$0.1N_i - 100$	16	2000	16	0.01	100
SF	yes	no	$0.9N_i$	100	$0.1N_i - 100$	8	3000	16	0.01	100
JL	no	yes	$0.9N_{all}$	100	$0.1N_{all} - 100$	–	–	32	0.001	50
JF	no	no	$0.9N_{all}$	100	$0.1N_{all} - 100$	–	–	32	0.001	50

Table 7. Hyper-parameters. N_i is the number of structures in the i -th species’ proteome, and N_{all} is the number of structures of all species. And max_node plays the similar role as batch_size, which represents the maximum number of residuals per batch.

A.2. Invariance

Experimental details For GraphTrans, StructGNN and GVP, we use their open-source PyTorch code without any changes. The platform for our experiment is ubuntu 18.04, with 8 Intel(R) Xeon(R) Gold 6240R Processors and 256GB memory. We use a single NVIDIA V100 to train and evaluate all models, where the CUDA version is 11.3 and Torch version is 1.10.1. To evaluate invariance, we retest pre-trained models (SL setting) on the test set that has been randomly rotated and translated. Besides, we provide the inference time of each model.

Results and analysis As shown in Table. 8, we conclude that GTrans, SGNN and ADesign are rotationally and translationally invariant considering the computational uncertainty. This property is determined at the feature level: all input features are invariant to rotations and translations. In contrast, GVP is equivalent, but not invariant, while the latter is what we really need for classification. In addition, ADesign is much faster than other methods during inference. However, the reported time includes model building and data loading and is not purely runtime, so it does not seem to be 40 times faster than the others.

	Raw data				Rotation+Translation				Inference time			
	GTrans	SGNN	GVP	ADesign	GTrans	SGNN	GVP	ADesign	GTrans	SGNN	GVP	ADesign
DANRE	51.8	52.5	<u>53.2</u>	63.5	51.9	<u>52.5</u>	42.6	63.7	21m30s	<u>19m37s</u>	1h30m58s	37s
CANAL	45.2	46.2	<u>48.5</u>	55.1	45.6	<u>46.0</u>	40.5	55.1	4m9s	<u>3m48s</u>	17m35s	13s
MOUSE	52.5	53.0	<u>55.0</u>	64.7	52.4	<u>53.1</u>	44.5	64.7	19m6s	<u>18m1s</u>	1h18m42s	37s
ECOLI	50.0	49.4	<u>51.9</u>	52.7	49.5	<u>50.0</u>	44.0	52.5	3m40s	<u>3m18s</u>	14m54s	18s
DROME	49.6	49.2	<u>51.2</u>	60.3	49.7	<u>49.6</u>	43.0	60.2	10m14s	<u>9m33s</u>	45m19s	24s
METJA	48.9	49.6	<u>50.9</u>	53.4	48.4	<u>49.3</u>	43.1	54.0	54s	<u>49s</u>	3m21s	10s
PLAF7	45.0	45.9	<u>48.6</u>	54.3	45.1	<u>45.8</u>	40.9	54.0	2m48s	<u>2m27s</u>	11m12s	12s
MYCTU	53.4	53.7	<u>56.9</u>	61.8	53.3	<u>53.7</u>	47.1	61.6	3m17s	<u>2m56s</u>	13m18s	13s
CAEEL	51.4	52.3	<u>54.1</u>	63.9	51.7	<u>52.1</u>	44.6	63.9	19m41s	<u>17m48s</u>	1h22m29s	39s
DICDI	49.7	50.2	<u>52.0</u>	61.4	49.4	<u>50.1</u>	43.6	61.1	8m47s	<u>8m0s</u>	36m29s	26s
TRYCC	52.4	52.5	<u>53.2</u>	65.7	52.1	<u>52.2</u>	43.8	65.7	17m31s	<u>14m40s</u>	1h11m27s	33s
YEAST	44.6	44.6	<u>48.9</u>	53.9	44.6	<u>44.8</u>	39.5	53.8	3m49s	<u>3m30s</u>	15m39s	14s
SCHPO	45.8	45.1	<u>47.8</u>	53.5	45.9	<u>45.1</u>	39.6	53.6	3m29s	<u>3m11s</u>	14m49s	17s
RAT	52.2	52.6	<u>53.8</u>	64.2	52.0	<u>52.6</u>	44.2	64.4	19m14s	<u>17m58s</u>	1h17m13s	39s
HUMAN	52.3	52.3	<u>53.8</u>	63.5	52.2	<u>52.3</u>	44.9	63.6	17m24s	<u>15m15s</u>	1h10m14s	33s
ARATH	52.3	53.2	<u>54.3</u>	65.1	52.3	<u>53.2</u>	45.0	65.1	28m42s	<u>24m27s</u>	1h55m27s	57s
MAIZE	54.1	54.9	<u>56.0</u>	67.9	54.1	<u>54.8</u>	43.7	67.8	39m25s	<u>33m25s</u>	2h43m43s	1m11s
LEIIN	47.6	48.8	<u>50.7</u>	57.5	47.8	<u>48.5</u>	42.8	57.5	5m19s	<u>4m53s</u>	21m54s	15s
STAA8	46.3	46.3	<u>48.7</u>	52.4	<u>46.0</u>	<u>46.0</u>	39.7	52.7	2m1s	<u>1m45s</u>	7m47s	12s
SOYBN	53.1	54.1	<u>55.6</u>	67.2	53.1	<u>54.0</u>	44.7	67.2	51m35s	<u>50m12s</u>	3h41m53s	1m41s
ORYSJ	55.2	56.3	<u>58.0</u>	69.5	55.1	<u>56.3</u>	42.2	69.5	40m58s	<u>35m15s</u>	2h52m11s	1m20s
Average	50.2	50.6	<u>52.5</u>	60.5	50.1	<u>50.6</u>	43.0	60.6	–	–	–	–

Table 8. Invariance. We retest pre-trained models (SL setting) on the test set that has been randomly rotated and translated. We also provide the inference time that includes model building and data loading.